LIMNOLOGY
AND
OCEANOGRAPHY

May 2000
Volume 45
Number 3

Limnol. Oceanogr., 45(3), 2000, 525–533

Advective particle transport into permeable sediments—evidence from experiments in an intertidal sandflat

Antje Rusch[1] *and Markus Huettel*
Max-Planck-Institute for Marine Microbiology, Celsiusstr. 1, D-28359 Bremen, Germany

Abstract

Advective transport of artificial and natural particles into permeable sediments was demonstrated in situ by field experiments in an intertidal Wadden Sea sandflat. Using dyed sediment, advective interfacial solute exchange was shown to reach down at least 1.5 cm below surface. Particle depth distributions depended on sediment permeability and particle size. Sandy sediments were found to efficiently trap particulate material. At the beginning of the local phytoplankton spring bloom, an average m^2 of coarse-grained sediment received 850-mg organic carbon per day by filtration of 14 liters of overlying water per hour. We discuss the relative importance of different transport mechanisms, and data from parallel studies on natural sediments at the same site are interpreted in close correlation to the results of the in situ experiment.

Deposition and resuspension are considered a major link between water column and the sediment (van Raaphorst et al. 1998), and on the inner shelf (water depth <100 m) suspended matter concentrations in the order of 0.1–1 g L^{-1} can occur (Eisma 1993). Here large amounts of inorganic and organic particulate matter are constantly involved in deposition/resuspension cycles, which move them into and out of the uppermost sediment layers. Friction velocities that are insufficient to cause resuspension may move particles in rolling or saltatory bedload transport (Dyer 1986). In rippled beds, material deposited on the surface is moved in the troughs toward the lee side of the ripples, where it tends to be buried by sand grains avalanching from the crest (Jenness and Duineveld 1985). Given this particular situation, the mixed depth of the sediment does not exceed the amplitude of the migrating ripples.

Apart from these purely hydrodynamic processes, biological activity also contributes to interfacial and subsurface transport. On a worldwide scale, biogeneous mixing, mainly due to deposit feeding (Wheatcroft et al. 1990), reaches down to a mean depth of 9.8 ± 4.5 cm (Boudreau 1998), with near-surface horizontal mixing rates by far exceeding vertical ones (Wheatcroft et al. 1990). Macrofaunal sediment reworking is generally considered the prevalent biogeneous mixing process, but in organically enriched muddy sediments the meiobenthos also can be important for the rapid and shallow initial burial of sedimented phytoplankton (Webb and Montagna 1993). Periodical irrigation of macrobenthos tubes and burrows enhances interfacial solute exchange (Forster and Graf 1995; Marinelli and Boudreau 1996; Ziebis et al. 1996*a*), and suspended particles are cotransported with the irrigation current.

Molecular diffusion generally dominates solute transport at the sediment surface (Glud et al. 1996), in cohesive sediments (Jørgensen 1996), and at burrow walls (Forster et al. 1996; Ziebis et al. 1996*b*). Over larger distances, however, convective water flows transport solutes and suspended particulate matter more efficiently. Percolation of sea water by tidal filling and draining of the porous sediment is important in the intertidal and the narrow subtidal zone (Riedl et al. 1972). In coastal wetlands, evaporation and infiltration fluxes are segregated by pore size (Harvey and Nuttle 1995). Convective flow after flooding is supported by water loss and warming during exposure and by a high permeability of the sediment (Rocha 1998).

The influence of surface waves is especially pronounced in shallow water areas (Eisma 1993). Internal waves, formed by various interactions of currents, bottom topography, surface waves, and tidal oscillations, can be much higher than surface waves (Kennish 1994) and may have comparable impact on the bottom of deeper waters on the outer shelf and shelf slope. Flow separations and persistent vortices, the

[1] Corresponding author (arusch@mpi-bremen.de).

Acknowledgments

M. Alisch and H. Tydt are gratefully acknowledged for their help during field work. The BAH Wadden Sea Station kindly provided laboratory space. We appreciate discussions and valuable comments of S. Forster and B. B. Jørgensen. The critical remarks of W. van Raaphorst and an anonymous reviewer helped to improve the manuscript. This study was supported by the Max Planck Society (MPG), and A.R. received a postgraduate scholarship from Deutsche Forschungsgemeinschaft (DFG).

dominant features in wave-induced oscillatory flows over sand ripples, provide an efficient mixing mechanism immediately above the sediment and enhance the vertical exchange of solutes between bottom and interstitial water (Shum 1995). Pressure variations along a rough permeable bottom, generated by the passage of currents or gravity waves, cause pore water circulation and increase solute fluxes across the sediment–water interface to an extent that depends on sediment permeability, ripple slope, wave height, and wavelength (Riedl et al. 1972; Shum and Sundby 1996).

Pressure-driven advective pore water flow into and out of permeable sediments is caused by the interaction of near-bottom currents and biogenic or physical sediment roughness (Huettel and Gust 1992*a*; Forster et al. 1996; Ziebis et al. 1996*b*). Interfacial fluid exchange depends on the permeability of the sediment (Huettel and Gust 1992*a*), flow velocity (Forster et al. 1996), and topography height (Huettel et al. 1996). In flume experiments, advective flow has been shown to increase oxygen penetration (Ziebis et al. 1996*b*) and use (Forster et al. 1996), as well as manganese, iron, and nutrient dynamics (Huettel et al. 1998). Advective co-transport of fluid and suspended particles across the water–sediment interface has been demonstrated in flume studies using 1- and 10-μm acrylic spheres (Huettel et al. 1996), 8-μm *Dunaliella* cells (Huettel and Rusch 2000), and *Thalassiosira weissflogii*, a diatom of 12-μm equivalent diameter (Pilditch et al. 1998). Moreover, field experiments have been conducted on phytopigment flux into coarse and fine sand (Pilditch et al. 1998), but results lacked depth resolution and were probably influenced by effects occurring near edges. Another approach to study advective interfacial particle transport in situ (Huettel and Rusch 2000) has proved flux and penetration depth of algae to depend on sediment permeability but failed to consider particle sizes. Nor were corresponding data of natural sediment from the same site available.

Advective transport of solutes and fine particles across the water–sediment interface, albeit well studied in the laboratory and probably important for early diagenesis in shallow water environments, has not received much attention in field studies yet. Our in situ experiments in an intertidal sandflat consider the validity of results from flume studies, mainly addressing the influence of sediment permeability and particle size on advective interfacial transport of (organic) particles. The understanding and interpretation of data on particulate organic matter (POM) dynamics at the same site (Rusch et al. in prep.) is improved by close correlation to the in situ experiment presented here. It contributes to the discussion on the ecological role of permeable shallow water sediments.

Methods

Study site—The field study was carried out in Königshafen (55°02′N, 008°26′E), an intertidal bay of Sylt Island (North Sea) with a mean tidal range of 1.7 m in its southern part (Austen 1997). Water temperatures range between −2°C and 23°C (Reise 1985), salinities from 23‰ in winter to 33‰ in summer (Kristensen et al. 1997). Near-bottom residual currents above the sandy tidal flats are weakly flood dominated (Austen 1994). For further details on Königshafen *see* Reise (1985).

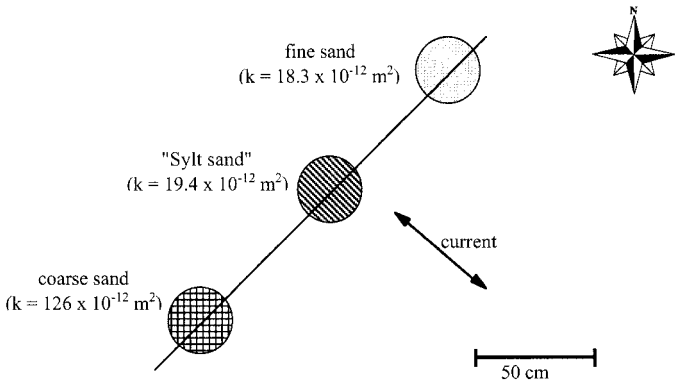

Fig. 1. Experimental setup of the microbead experiment. Arrow indicates the prevailing current direction in the study area.

Experiments were conducted 250 m offshore on a tidal flat in southern Königshafen, where bottom topography consisted mainly of 1–3-cm high ripples and the predominant direction of tidal currents was southeast/northwest. Benthic macrofauna was comparable to that of sandflats with short exposure time, which were thoroughly studied by Reise et al. (1994). During the experiments in March 1998, current velocities at 2 cm above the bottom did not exceed 0.10 m s^{-1}, waves were smaller than 0.2 m, and a phytoplankton bloom dominated by *Brockmanniella brockmannii* and *Skeletonema costatum* had recently started. Sediment permeabilities, measured in cores of 60 mm inner diameter using the constant head method (Klute and Dirksen 1986), ranged between 18 and 94 $\times$ 10^{-12} m^2 in the uppermost 4 cm and between 18 and 52 $\times$ 10^{-12} m^2 in 4–8-cm depth. Median grain sizes in these depth intervals were 460–500 and 390–460 μm, respectively.

Dye experiment to assess the depth of advective solute exchange—Three sediment cores (36-mm diameter, 10-cm long) were taken from the study site. After staining the pore water with rhodamine, we reinserted the cores into wells, which had been cut into the sediment using equal-sized tubes, and removed the coreliners. During the procedure, no visible loss of the strongly dyed pore water occurred. Two days (i.e., four tidal cycles) later the cores were retrieved, and the depth of dye removal was assessed visually.

Microbead experiment to investigate interfacial particle transport—Two hours before low tide, three artificial sand cores (28-cm diameter, 20-cm depth) were carefully inserted into the natural sediment as shown in Fig. 1, according to the following procedure: the PVC coreliners, on the bottom side tightly covered by polyethylene sheets, were embedded in narrow wells and fixed by carefully consolidating the surrounding sand. Then they were filled half with particle-free local seawater before adding cleaned marine sand until the saturated cores were level with the surrounding sediment. To ensure equal environmental conditions, we aligned the cores within 2 m, with the line perpendicular to the main current direction to avoid particle cross contamination. We used cleaned marine coarse sand (grain size 500–1,000 μm), fine sand (grain size 125–250 μm), and Sylt sand (grain size

median: 655 μm), i.e., sediment from a sandy site nearby that had been collected in September 1997, washed, and oven dried.

Fluorescent microbeads (1-, 3-, and 30-μm diameter; Duke Scientific) were suspended in particle-free local seawater and poured around the edges of the cores in a ring of 2.5-cm width using a template. Particle densities were $(2.60 \pm 0.98) \times 10^{12}$ m^{-2}, $(1.34 \pm 0.34) \times 10^{11}$ m^{-2}, and $(2.56 \pm 0.70) \times 10^{8}$ m^{-2} for the blue (1 μm), red (3 μm), and green (30 μm) beads, respectively. Finally, we carefully removed templates and coreliners.

After 13 h (1.5 h before the next low tide), five cores (60-mm diameter) were taken from each artificial core using Plexiglas® tubes; central ones were named A/B/C, marginal ones D/E. At the same time, the water column was sampled nearby using PE bottles, providing six parallels of 250 ml each. These samples were preserved by addition of glutaraldehyde (2% final concentration) and stored at 4°C.

Pretest to estimate sampling bias—Seven cubic decimeters of each sand type described above were saturated with particle-free sea water in a bucket. Aliquots of the microbead suspension used in the main experiment were spread over the artificial sediment surfaces (particle density: 1/100 compared to the field study) and allowed to settle for 10 min. Then we took three cores (60-mm diameter) from each bucket to quantify any particle movement not induced by natural currents.

Sample treatment—After 8 h storage at 4°C, the cores were sliced into 1-cm sections down to 20 cm (pretest cores: 7 cm) depth. Each slice was carefully suspended in NaCl solution (32‰) and allowed to settle for 20 s to separate fine particles ($<$70 μm). The resulting suspensions (ca. 40 ml) were decanted into screw-cap or snap-lock glasses, the remaining sediment was once more retreated alike. After addition of glutaraldehyde (2% final concentration) the suspensions were stored at 4°C.

Analyses

Two aliquots (equivalent to 1/80–1/3) of each sample, including the water samples, were filtered on polycarbonate filters (0.8-μm pore size; Millipore ATTP) applying gentle vacuum. The filters were examined by epifluorescence microscopy (Zeiss Axioskop), using a magnification of 100 times for counting the green beads and 400 or 1,300 times for counting the red and blue ones. On each filter, each bead type was scored in five counting grids; in the case of very few green beads, the complete filter was scanned.

Two more aliquots of 50–200 μl of sample were stained with 4′,6-diamidino-2-phenylindole (DAPI) and filtered on polycarbonate filters (0.2-μm pore size, Millipore GTBP) applying gentle vacuum. On each filter, epifluorescent bacteria were scored in five counting grids using a magnification of 1,300 times.

Diatom numbers and lengths $>$10 μm were obtained using a Fuchs/Rosenthal chamber and a magnification of 400 times. We scored benthic and planktonic forms (Pankow 1990), each sorted into five length classes (10–15, 15–20, 20–25, 25–30, $>$30 μm).

Statistics

All statistics were performed according to Sachs (1997). We applied the Kruskal/Wallis test, the Lord test, the estimation of standard deviations from the range of values and the (small) number of parallels, and the Wilcoxon matched pairs signed rank test.

The Kruskal/Wallis test is performed as a rank test to find out if a group of random samples belong to a common total set. We had three random samples (sand types) of five observations (subcores) each. Possible differences between the sand types with respect to the depth distribution and penetration depth of certain particles were examined for significance using the Kruskal/Wallis test. It was applied to microbeads in the pretest and to microbeads and diatoms in the main experiment.

After detecting a significant difference by Kruskal/Wallis, we compared the sand types by pairs using the Lord test. This test is analogous to the Student *t*-test and compares the mean values of two small ($n \leq 20$) random samples using ranges instead of standard deviations as a measure of variation. We applied the Lord test to the depth distribution and penetration depth of microbeads of each bead size. Moreover, this test was used for each sand type to compare planktonic and benthic diatoms of different size classes with respect to their depth distribution and penetration depth.

For small numbers of parallels (usually $n < 15$), standard deviations must be estimated from the range of values using a factor tabulated in literature. We applied this procedure to the particle penetration depths given in Table 3. The Wilcoxon matched pairs signed rank test is used to find out whether the differences within the pairs are distributed symmetrically around a median of zero. For a given pair of particle sizes, each of our 15 cores provided a pair of observations, formed by the two corresponding depth distributions or penetration depths. Applying this rank test, we set up an order of particle types with respect to particle shares below 1-cm depth and to penetration depths.

In a strict sense, the subcore parallels are not statistically independent and the tests described above are therefore not applicable to our data set. The experiment would have to be conducted at least in duplicate or triplicate to gain a suitable data set allowing for statistically proven results. Hence, the outcomes of our statistical analyses should be regarded as probable trends, keeping in mind that their significance indispensably requires the subcores to be independent parallels.

Results

Dye experiment—No rhodamine was visible in the uppermost 1.0–1.5 cm of the cores that had been exposed to calm conditions for 2 d. The boundary toward the strongly dyed sediment below was slightly blurred (Fig. 2).

Pretest—Significant differences in particle depth distribution between the different sediment types could not be detected for any bead size (Kruskal/Wallis test). Thus, depth

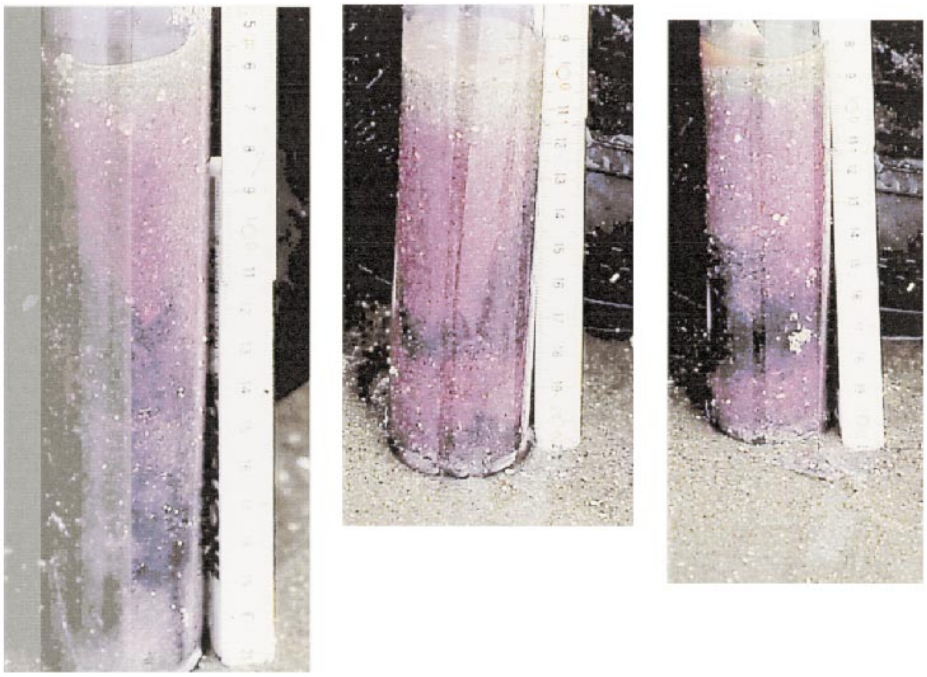

Fig. 2. Retrieved cores of the dye experiment.

distributions in the main experiment were directly comparable to each other.

Microbead experiment—After their exposure to tidal inundation, the surfaces of the artificial cores were still distinct from the adjacent sediment and unaffected by visible particle deposition and lateral sediment movement. Neither the artificial cores nor the surrounding natural sediment had a rippled surface. Transient formation of small ripples during high tide, however, was likely in spite of the calm weather. No macrofauna was found in the sliced cores.

Retrieval of microbeads, averaged over the sizes, was 9.3% of the deployed tracer particles in the coarse sand, 0.6% in the fine sand, and 1.0% in the Sylt sand. Depth-integrated numbers of microbeads in all parallel cores of the different sediment types are given in Table 1. The beads were not evenly distributed over the areas of the artificial cores. For each sand type, we considered the three subcores that received most tracer particles, and neither of these sets contained all central cores (A, B, C) or all marginal ones (D, E), but two central and one marginal core each.

In the following, particle depth distributions are treated in terms of relative particle numbers, i.e., numbers within a depth interval divided by the depth-integrated total of the respective profile. Figure 3 shows depth distributions of different artificial and natural particles found in the coarse, fine, and Sylt sand cores. Differences between these sand types with respect to relative particle numbers were detected (Kruskal/Wallis test) for the green (α = 5.1%), red (α = 0.9%), and blue microbeads (α = 4.9%), as well as for 10–15-μm benthic diatoms (α = 6.7%) and for 15–20-μm benthic (α = 4.8%) and planktonic diatoms (α = 10.5%). The latter consisted mainly of the bloom-forming *B. brockmannii*. Moreover, microbeads depth distributions were compared by pairs (Lord test); the results are compiled in Table 2. Bacteria appeared to penetrate deeper into coarse than into fine sand (Fig. 3), statistical confirmation lacked parallel counts, though.

No significant difference in the depth distributions of diatoms could be detected (Lord test), neither between planktonic and benthic algae of the same size nor between different size classes of planktonic diatoms. For the following

Table 1. Depth-integrated numbers of microbeads retrieved in coarse, fine, and Sylt sand. Green beads: $\times 10^3$, red beads: $\times 10^6$, blue beads: $\times 10^7$. A–E: parallel cores.

Sand type	Beads	A	B	C	D	E
Coarse (500–1000 μm)	30 μm (green)	24.0	0.37	95.2	0.16	6.61
	3 μm (red)	24.9	3.93	44.2	0.21	12.4
	1 μm (blue)	29.3	1.84	47.5	0.28	12.9
Fine (125–250 μm)	30 μm (green)	0.42	1.03	0.99	0.11	1.37
	3 μm (red)	0.34	0.50	0.58	0.22	0.32
	1 μm (blue)	0.42	0.83	1.16	0.38	0.63
Sylt (median: 655 μm)	30 μm (green)	0.36	0.11	0.06	0.03	22.1
	3 μm (red)	0.37	0.18	0.25	0.13	6.00
	1 μm (blue)	0.26	0.23	0.26	0.13	4.93

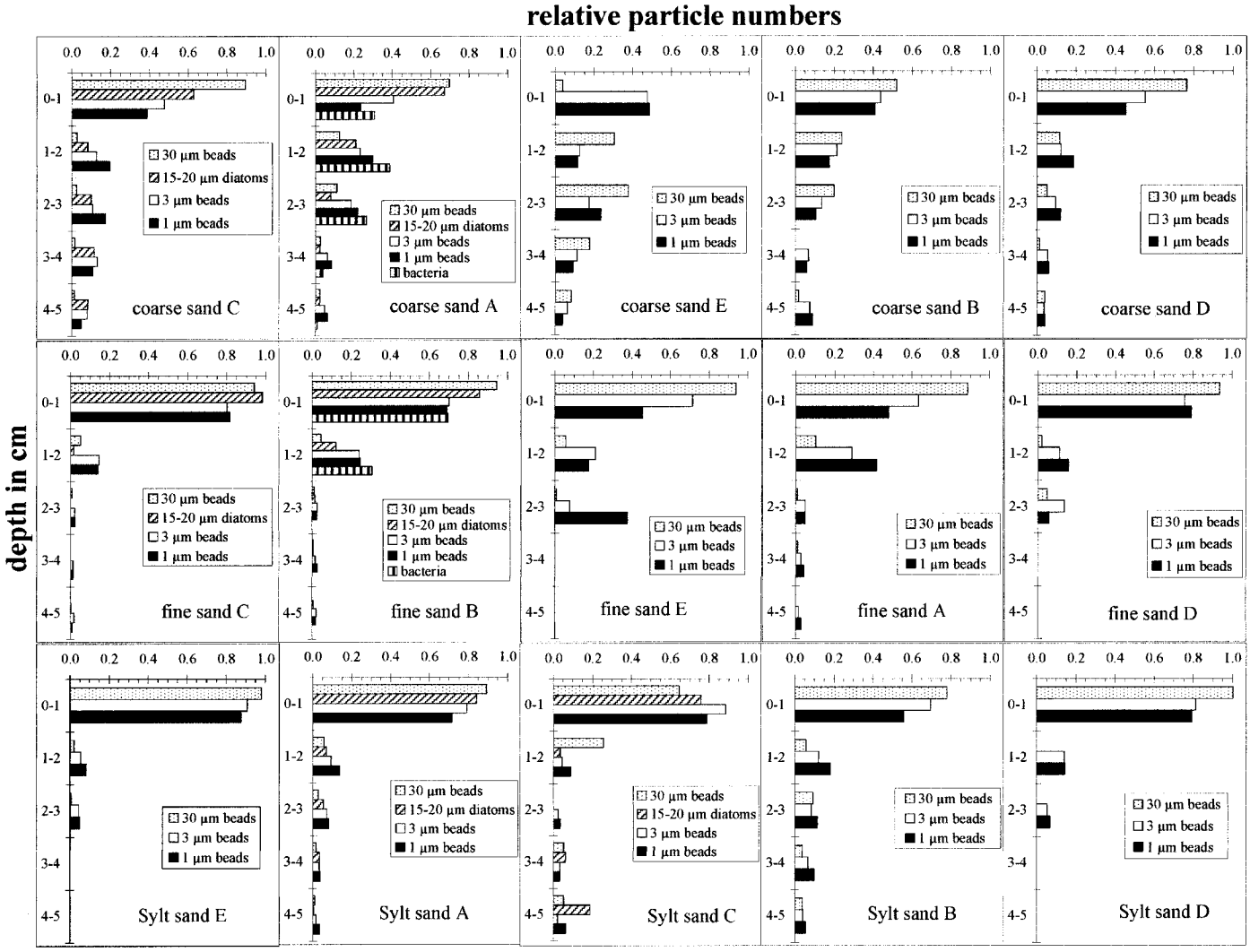

Fig. 3. Depth distributions of microbeads (30 μm stippled, 3 μm white, 1 μm black), planktonic diatoms (15–20 μm hatched), and bacteria (striped) in terms of relative particle numbers in coarse, fine, and Sylt sand cores. Within a row, the panels are arranged with respect to the total number of beads found in the corresponding parallel cores (cf. Table 1). Profiles from particle-rich and particle-poor cores are shown at the left and at the right, respectively.

tests we averaged planktonic diatom numbers over all size classes and compared them to the corresponding relative particle numbers of the microbeads. The share of particles penetrating deeper than 1 cm was in the order (α = 5%, Wilcoxon matched pairs signed rank test): blue beads (1 μm) > red beads (3 μm) > green beads (30 μm) ≈ diatoms (>10 μm). Relative numbers of bacteria (0.5–1 μm) appeared similar to that of the blue beads, though without statistical confirmation.

Table 2. Levels of significance (Lord test) of differences between particle depth distributions. n.s.: not significant ($\alpha > 5\%$).

	30 μm (green)	3 μm (red)	1 μm (blue)
Coarse vs. fine	5%	1%	5%
Coarse vs. Sylt	n.s.	1%	1%
Fine vs. Sylt	n.s.	n.s.	n.s.

In nearly all profiles (exception: 30-μm beads in coarse sand E), relative particle numbers decreased exponentially with depth. The mean correlation coefficients were r^2 (beads) = 0.848 and r^2 (diatoms) = 0.668. The penetration depth was defined as corresponding to a decrease of relative particle numbers by a factor e^{-3}, i.e., 5.0% of the surface value. The penetration depths of microbeads, diatoms, and bacteria in each sand type are summarized in Table 3. Red (3 μm) and blue microbeads (1 μm) penetrated significantly deeper into coarse sand than into fine and Sylt sand (α = 1%, Lord test). Green microbeads (30 μm) penetrated deeper into coarse sand than into fine sand (α = 1%, Lord test), but no significant differences to the Sylt sand were detected (α = 5%, Lord test).

No significant difference could be detected (Lord test) between the penetration depths of diatoms of different size classes. So the penetration depths of planktonic diatoms were averaged over all size classes and compared to the corresponding ones of the microbeads. The penetration

Table 3. Penetration depths (in cm, mean of parallel cores) of differently sized particles in coarse, fine, and Sylt sand. As penetration depths of diatoms did not significantly differ between the size classes, they were averaged. Standard deviations were estimated according to Sachs (1997) from the range of values and the number of parallels.

	Coarse sand (500–1000 μm)	Fine sand (125–250 μm)	Sylt sand (median: 655 μm)
30-μm beads	2.83 ± 0.54	1.33 ± 0.22	2.35 ± 1.38
Diatoms (>10 μm)	3.04 ± 0.19	2.11 ± 0.29	2.19 ± 0.29
3-μm beads	5.27 ± 0.68	2.53 ± 0.19	2.62 ± 1.03
1-μm beads	5.32 ± 0.77	2.59 ± 0.46	3.10 ± 1.44
Bacteria	2.51 (1 core)	3.66 (1 core)	n.d.

depths were in the order (α = 5%, Wilcoxon matched pairs signed rank test): blue beads (1 μm) > red beads (3 μm) > green beads (30 μm) ≈ diatoms (> 10 μm). Bacteria (0.5–1 μm) appeared to penetrate approximately as deep as the blue and red beads, though without statistical confirmation.

The biovolume of planktonic diatoms, i.e., their abundance in a certain size class multiplied by the corresponding average cell volume, summed over all size classes, was determined. In the coarse sand (cores A, B, C) down to 5-cm depth it amounted to 4.97 cm^3 (m^2 sediment)$^{-1}$. Provided that the cells had a density of 1.1 g cm^{-3} and a water content of 0.8 (w/w), and that they got into the sediment within 13 h, the POM transport rate was 2.02 g (dry weight) m^{-2} d^{-1}. With particulate organic carbon (POC) ≈ 0.42 × POM (Rice et al. 1986), this corresponds to a net POC input rate of 850 mg C_{org} m^{-2} d^{-1}.

The number of planktonic diatoms in the coarse sand (cores A, B, C) down to 5-cm depth that were filtered from the water by 1 m^2 of sediment during the experiment equaled the number in 178 ± 74 liters of bottom water. These calculations depend on the diatom size class with net filtration rates increasing with the size of diatoms. Assuming that this water volume had been passed through the sediment within the 13 h of the experiment, and furthermore assuming steady state, we obtained net areal filtration rates of 13.7 ± 5.7 liters m^{-2} h^{-1}. These estimates are net rates, as interfacial water flows carry particles not only into, but also out of the sediment.

Discussion

Interfacial POM transport is an important link between the biogeochemical cycles of the water column and the sediment. Our in situ experiments were designed to assess magnitude and depth penetration of advective interfacial particle transport. We first discuss several generally important transport mechanisms with respect to their possible impact on our experimental results, followed by detailed considerations on the observed features of advective transport: horizontal heterogeneity, influence of sediment permeability, and influence of particle size. Our experimental data are compared to the results of earlier laboratory studies and measurements in natural sandy sediments. Finally, we discuss the implications of advective interfacial transport on the cycling of organic matter in marine ecosystems.

Contribution of nonadvective particle transport—We showed particle transport into sandy sediments within one tide, which generally could have been facilitated by various processes. Biogeneous transport was hardly contributing, as no macrofauna was found in the cores. Particles deposited on the sediment surface were not buried deeply by migrating sand ripples either, as only small ripples could form due to the quite calm current regime during the experiment. Nor could tidal percolation trap the microbeads, because ebb tide began 8 h after the start of the experiment, i.e., more than 5 h after inundation of the study site, and during that time suspended beads would have been swept far away. Particles already trapped in the sediment at the onset of ebb tide, though, could have received some additional drag downward by falling water levels. Convective flow caused by evaporation and warming during exposure did not apply for this experiment, because the site was exposed for less than 3 h and the sediment surface temperature was 6°C, differing from that of air, water, and deeper sediment layers by less than 1°C. During exposure the wind speed was 3.4–4.3 m s^{-1}, corresponding to a wind force of 2–3 Bft. (Deutscher Wetterdienst, unpubl. data), so evapotranspiration was negligible, too.

Dye experiments show advective solute exchange—The result of our dye experiment was the combined effect of bedload transport, resuspension/redeposition, and advection. Under the calm hydrodynamic conditions, however, lateral transport and resuspension of the relatively coarse grains were negligible. The sediment, comparable to the Sylt sand used in the microbead experiment, was sufficiently permeable for advective pore water flow (*see below*), and dye removal reaching 1.5 cm down into the sediment thus can be attributed to advective interfacial water exchange. Mixing in the interstices may have added to the dye removal by causing a dilution of the stained pore water. However, the strong color of rhodamine is visually well perceptible even when diluted by a factor of 200 compared to our staining solution. Flushing the sediment with a water volume exceeding 200 times its pore volume within only 2 d was hardly probable. Diffusion and interstitial mixing could be responsible for the blurred boundary between stained and clean sediment, but fail to explain the whole observation. As the main process we rather consider advective flow pushing the stained water out of the cores without needing large water volumes. The deformation of dyed vertical pore water stripes in an even finer grained sandy sediment (220 μm) exposed for merely 3 h to flume water currents slower than 0.1 m s^{-1} (Huettel and Gust 1992*a*) showed that rhodamine dye is pushed along the pathway of advective pore water flow by the intruding and advancing front of bottom water. In finer grained sediments, like the artificial fine sand we used, advective flushing is relatively slow due to lower permeabilities, and resuspension gains importance, as smaller grains are more easily suspended. By contrast, in coarser grained sediments, like our artificial coarse sand, the relatively high permeabilities are expected to facilitate extensive advective flows, whereas resuspension becomes less influential.

We conclude that the Königshafen sediments permitted advective flushing and that the main particle transport process in the microbead experiment was most likely advection,

too, although the two experiments were not conducted on the same day.

Horizontal heterogeneity in the microbead experiment—Each of the three artificial cores exhibited horizontal heterogeneity, which was consistent between all bead sizes and not related to the distance from the core edge (Table 1). This uneven distribution could be due to areas of high and low pressure created by the interaction of currents with bottom roughness. Such pressure fields have been shown in laboratory flumes for topography heights of 5–28 mm (Huettel and Gust 1992*a*; Forster et al. 1996; Huettel et al. 1996; Ziebis et al. 1996*b*) and 70 mm (Pilditch et al. 1998). As the principle also applies to smaller topographic structures, bottom roughness and temporary ripples during our field experiment were apparently sufficient to cause pressure heterogeneities as the driving force for water and particle flows. Profiles from the coarse sand cores that trapped many particles (Table 1) showed subsurface maxima, e.g., microbeads of all sizes in core E, 1-μm microbeads and bacteria in core A, and 15–20-μm planktonic diatoms in core C (Fig. 3), as well as 10–15-μm planktonic diatoms in core C (Huettel and Rusch 2000). These profiles reflect the history of the cores with respect to pressure fields moving over them. When exposed to locally high pressure, the sand was advectively supplied with particles, whereas subsequent exposure to low pressure caused an upwelling of pore water. Apparently only close to the surface, its velocity was sufficient to overcome friction, suspend, and move particles (Huettel et al. 1996). Another phase of high pressure may enter particles in the top layers again. In core E, the second deposition may have started late during the experiment, when ebb current velocities had already decreased below the threshold for remobilization of 30-μm beads from the surrounding sediment. In core A, only small particles were affected, indicating that this area experienced weaker pressure changes, insufficient to move larger particles upward. In core C, only diatoms were slightly more abundant in 3–4-cm depth than in 1–3-cm depth. If this subsurface maximum is significant at all, it might be caused by active rather than passive movements of the algae. Profiles from coarse sand cores that trapped fewer particles (Table 1) were at first located in low pressure areas and later on received particles once, their relative numbers thus decreasing exponentially with depth (Fig. 3).

Besides pressure changes, concentration changes or a patchy distribution of particles in the bottom water also are equally reasonable explanations for the observed profiles. Temporal and spatial variations of suspended particle concentrations can be caused by changes in tidal current velocity or by heterogeneous pressure fields.

Fine and Sylt sand cores probably were also exposed to migrating pressure/concentration fields (or pressure/concentration changes at a given location). Owing to their lower permeability, however, advective transport was too slow to cause measurable changes in the particle profiles within 10 h of inundation. Natural sandy sediments are constantly subject to changing flow and pressure fields, and given enough time, advectively accumulate fine-grained material in subsurface layers, even if they are less permeable than our artificial coarse sand. Natural cores taken from the same study site between July 1997 and July 1998 contained maximum concentrations of particles <70 μm in 4–8-cm depth (Rusch et al. 2000, in prep.).

Sediment permeability as a key factor in advective transport—Our in situ experiment showed how particle transport into and in the sediment depends on the permeability of the sediment. In the coarse sand, we retrieved 1 order of magnitude more microbeads than in the fine and Sylt sands, and artificial as well as natural particles penetrated deeper into the coarse than into the less permeable sands (Fig. 3). Laboratory studies in flumes and stirred chambers have shown that highly permeable sediments compared to less permeable ones exhibit stronger and deeper reaching influx (Forster et al. 1996) and efflux of dyed water (Huettel and Gust 1992*a*, 1992*b*), deeper penetration of oxygen (Ziebis et al. 1996*b*), more intense oxygen use (Forster et al. 1996), and larger deposition of diatoms to the bed (Pilditch et al. 1998). Our in situ experiment demonstrated that interfacial fluxes and particle penetration depths are also increased by high permeabilities when the sediment is exposed to a natural environment. Experiments in stirred chambers have shown that interfacial particle fluxes, penetration depths, and sedimentary degradation of the trapped algal cells depended on the logarithm of sediment permeability (Huettel and Rusch 2000). This key factor of advective transport is influenced not only by the grain size of the sediment, but also by its sorting and state of consolidation, animal burrows, benthic diatom mats, or bacterial mats in the so-called versicolored sandy tidal flats (Krumbein et al. 1994). Moreover, the advectively caused subsurface accumulation of fine-grained material reduces the permeability of the affected sediment layer, hence decelerating the pore water flow and enhancing further deposition of the particles it carries. The degradation of organic fines, in permeable sediments enhanced by advective oxidant supply, restores and maintains the long-term nonaccumulating feature and high permeability of sandy sediments. Enhanced organic matter turnover may give rise to the formation of subsurface microbial biofilms, which in turn decrease sediment permeability. Occasional erosion during stormy weather limits the persistence of such biofilms and therefore may be an important process in keeping the uppermost centimeters highly permeable. Contrasting our artificial sands, permeability in natural sediments is horizontally and vertically heterogeneous, resulting in internal interfaces that modify the flow and pressure field. Besides, natural sands are less well sorted, ensuring a different spectrum of pore sizes. Therefore our Sylt sand was only as permeable as our fine sand in spite of its much higher median grain size.

The minimum permeability needed for advective interfacial fluxes of water and microalgae was 1×10^{-12} m^2 (Huettel and Gust 1992*a*) and 1.5×10^{-12} m^2 (Huettel and Rusch 2000), respectively. This threshold corresponds to a relatively well-sorted fine sand (Huettel and Gust 1992*b*). As a consequence of the shallow water hydrodynamic regime, permeable sands are the prevailing sediment type on the continental shelves (Emery 1968; Riedl et al. 1972). These areas are consequently important stages for advective interfacial transport to act on.

The role of particle size—Particles penetrated deeper the smaller they were. Within the diatoms, depth distributions did not significantly depend on particle size because depth

resolution was insufficient to reveal differences between particles that hardly penetrated into the second slice of the cores. On average, though, their depth distribution agreed well with that of the similarly big green beads and therefore supported the finding of size-related particle penetration. Flume studies have shown the following order of penetration depths in permeable sediments: fluid > 1-μm particles > 10-μm particles (Huettel et al. 1996). Our in situ experiment demonstrated that the penetration depth of advectively moved particles also depends on their size, when the sediment is exposed to a natural environment. It further showed that naturally occurring particles like diatoms and bacteria fit well into the results derived from artificial particles. The calculation of penetration depths from the exponential decrease of relative particle numbers is an attempt to put into numbers the qualitative statements derived from the significantly different particle depth distributions and additional visual evaluation of the profiles. Although it may be an oversimplification and prone to errors, careful consideration of both approaches probably yields reliable statements. From intuition and flume study results (Huettel et al. 1996) fluids are expected to penetrate deeper than particles. So water penetration down to 1.5 cm in the dye experiment (Fig. 2) seems to be at odds with particle penetration 2–3 cm down into the Sylt sand (Table 3). The two experiments, however, are not directly comparable to each other, as they were conducted on different days. Besides, the stained sand had not received the same pretreatment as the Sylt sand, resulting in slightly different permeabilities. Furthermore, detection methods were different. With three-quarters of even the smallest tracer particles being trapped within the first centimeter of their way downward (Fig. 3), interstitial flow velocities in the Sylt sand apparently decreased drastically in the uppermost layers. Decelerated advective flows deeper down could move small water volumes, sufficient to be traced by the particles they carried, but insufficient to push away major volumes of dyed pore water. Additionally, at the boundary between the stained and the advectively destained layers, a steep concentration gradient arose, and rhodamine could diffuse upward, thus decreasing the apparent fluid penetration depth in the dye experiment.

Rates and velocities of interfacial particle transport—The mean net rate of bottom water filtration by the sediment calculated from our diatom data was (13.7 ± 5.7) L m^{-2} h^{-1} and, thus, slightly exceeded areal filtration rates of 0.5–6.8 L m^{-2} h^{-1} derived from laboratory experiments with smooth sediments exposed to water flows in flumes (Huettel and Gust 1992*a*,*b*; Huettel et al. 1996; Pilditch et al. 1998). These reported data points, however, were scattered over a broad range of grain sizes (170–1,200 μm), flow velocities (1–10 cm s^{-1}), and run times (5 h–7 d), covering all but matching none of our experimental conditions. Thus, dealing with 3 degrees of freedom, more precise comparisons seem idle. Filtration rates calculated from planktonic diatom numbers tended to increase with cell size. Big diatoms may settle faster onto the sediment surface and be less easily resuspended than smaller ones. This difference in surficial net deposition rates could influence the relative distribution of cells in the water column and the sediment that our calculations were based on.

Within 13 h, particles penetrated at least 5 cm into our sediment cores, corresponding to a mean transport velocity of 3.8 mm h^{-1}. Vertical tracer velocities in the order of mm h^{-1} were also found in flume studies on smooth sediments under similar conditions (Huettel and Gust 1992*a*; Huettel et al. 1996). Not only topography and sediment permeability strongly influence the vertical progress of fluid and particles, but also the position in the pressure field (Huettel et al. 1996). In the field, the bottom currents change throughout the tidal cycle, thus adding further variability to the advective interfacial and subsurface flow velocities. Moreover, stronger bottom currents can cause the formation and migration of sand ripples. The resulting horizontal movement of the nonstationary flow field triggers additional temporal variability at a given spot.

Conclusions

We have shown in an intertidal sandflat that advective interfacial flows carry suspended planktonic and benthic diatoms, as well as bacteria and artificial tracer particles, into permeable sediments. We found horizontal heterogeneity and an impact of sediment permeability and particle size. Several profiles showed clear signs of alternating exposure to high and low pressure and resembled fine particle profiles from natural sediments of the same study site. Our in situ experiment gives clear evidence that advective particle transport is involved in the biogeochemical budgets of sandy shelf sediments. The extent of this advective influence relative to other transport processes depends on the ecosystem under consideration. In densely populated intertidal or subtidal areas, bioturbation and bioirrigation may dominantly contribute to interfacial particle and solute fluxes. However, macrofauna also can enhance advective exchange by increasing the permeability, the water–sediment interface area, and surface topography (Forster and Graf 1995; Marinelli and Boudreau 1996; Ziebis et al. 1996*a*). Shallow water sediments are strongly influenced by gravity waves and bottom currents and are well supplied with particulate organic matter from the euphotic zone. Therefore they are important sites of benthic mineralization to an extent that would not be possible without advective transport across and below the water–sediment interface. Recurrent resuspension and redeposition of the uppermost sediment layers gain more importance the finer the sand. Advective flows become slower and thus less effective, and the sediment gets more selective with respect to particle size and shape. Nevertheless, dissolved oxidants, bacteria, and very fine-grained or dissolved organic matter may penetrate sufficiently deep into fine sands to ensure an advectively caused increase of the sedimentary mineralization capacity.

From the diatom transport into the coarse-grained artificial core we roughly estimated an advective POC input rate of 850 mg C_{org} m^{-2} d^{-1}. Mineralization rates of sandy North Sea sediments range between 10 and 555 mg C m^{-2} d^{-1} (Canfield et al. 1993; Upton et al. 1993; Kristensen and Hansen 1995; Osinga et al. 1996; Boon and Duineveld 1998); in natural sands from our Königshafen study site we measured seasonally varying rates between 20 and 580 mg C m^{-2} d^{-1} (unpubl. data). Thus, mineralization and advective input of organic carbon were in the same order of magnitude, emphasizing the important role of advective interfacial transport for the carbon turnover in sandy shelf sediments. Con-

sidering that not only carbon, but all kinds of solutes and fine-grained particulate materials are to some extent advectively exchanged between the water column and the sediment, hydrodynamic processes may codetermine the benthic ecology of the uppermost ca. 5 cm of sandy shallow water sediments.

References

AUSTEN, G. 1994. Hydrodynamics and particulate matter budget of Königshafen, southeastern North Sea. Helgol. Meeresunters. **48:** 183–200.

AUSTEN, I. 1997. Temporal and spatial variations of biodeposits—a preliminary investigation of the role of fecal pellets in the Sylt-Rømø tidal area. Helgol. Meeresunters. **51:** 281–294.

BOON, A. R., AND G. C. A. DUINEVELD. 1998. Chlorophyll *a* as a marker for bioturbation and carbon flux in southern and central North Sea sediments. Mar. Ecol. Prog. Ser. **162:** 33–43.

BOUDREAU, B. P. 1998. Mean mixed depth of sediments: The wherefore and the why. Limnol. Oceanogr. **43:** 524–526.

CANFIELD, D. E., B. THAMDRUP, AND J. W. HANSEN. 1993. The anaerobic degradation of organic matter in Danish coastal sediments: Iron reduction, manganese reduction, and sulfate reduction. Geochim. Cosmochim. Acta **57:** 3867–3883.

DYER, K. R. 1986. Coastal and estuarine sediment dynamics. Wiley.

EISMA, D. 1993. Suspended matter in the aquatic environment. Springer.

EMERY, K. O. 1968. Relict sediments on continental shelves of world. Am. Assoc. Pet. Geo. Bull. **52:** 445–464.

FORSTER, S., AND G. GRAF. 1995. Impact of irrigation on oxygen flux into the sediment: Intermittent pumping by *Callianassa subterranea* and ''piston pumping'' by *Lanice conchilega.* Mar. Biol. **123:** 335–346.

———, M. HUETTEL, AND W. ZIEBIS. 1996. Impact of boundary layer flow velocity on oxygen utilization in coastal sediments. Mar. Ecol. Prog. Ser. **143:** 173–185.

GLUD, R. N., S. FORSTER, AND M. HUETTEL. 1996. Influence of radial pressure gradients on solute exchange in stirred benthic chambers. Mar. Ecol. Prog. Ser. **141:** 303–311.

HARVEY, J. W., AND W. K. NUTTLE. 1995. Fluxes of water and solute in a coastal wetland sediment. 2. Effect of macropores on solute exchange with surface water. J. Hydrol. **164:** 109–125.

HUETTEL, M., AND G. GUST. 1992*a*. Impact of bioroughness on interfacial solute exchange in permeable sediments. Mar. Ecol. Prog. Ser. **89:** 253–267.

———, AND ———. 1992*b*. Solute release mechanisms from confined sediment cores in stirred benthic chambers and flume flows. Mar. Ecol. Prog. Ser. **82:** 187–197.

———, AND A. RUSCH. 2000. Transport and degradation of phytoplankton in permeable sediment. Limnol. Oceangr. **45:** 534–549.

———, W. ZIEBIS, AND S. FORSTER. 1996. Flow-induced uptake of particulate matter in permeable sediments. Limnol. Oceanogr. **41:** 309–322.

———, ———, ———, AND G. W. LUTHER III. 1998. Advective transport affecting metal and nutrient distributions and interfacial fluxes in permeable sediments. Geochim. Cosmochim. Acta **62:** 613–631.

JENNESS, M. I., AND G. C. A. DUINEVELD. 1985. Effects of tidal currents on chlorophyll *a* content of sandy sediments in the southern North Sea. Mar. Ecol. Prog. Ser. **21:** 283–287.

JØRGENSEN, B. B. 1996. Material flux in the sediment, p. 115–135. *In* B. B. Jørgensen and K. Richardson [eds.], Eutrophication in coastal marine ecosystems. American Geophysical Union.

KENNISH, M. J. 1994. Practical handbook of marine science, 2nd ed. CRC.

KLUTE, A., AND C. DIRKSEN. 1986. Hydraulic conductivity and diffusivity: Laboratory methods, p. 687–700. *In* A. Klute [ed.], Methods of soil analysis—part 1—physical and mineralogical methods. American Society of Agronomy.

KRISTENSEN, E., AND K. HANSEN. 1995. Decay of plant detritus in organic-poor marine sediment: Production rates and stoichiometry of dissolved C and N compounds. J. Mar. Res. **53:** 675–702.

———, M. H. JENSEN, AND K. M. JENSEN. 1997. Temporal variations in microbenthic metabolism and inorganic nitrogen fluxes in sandy and muddy sediments of a tidally dominated bay in the northern Wadden Sea. Helgol. Meeresunters. **51:** 295–320.

KRUMBEIN, W. E., D. M. PATERSON, AND L. J. STAL. 1994. Biostabilization of sediments, Bibliotheks- und Informationssytem der Universität Oldenburg.

MARINELLI, R. L., AND B. P. BOUDREAU. 1996. An experimental and modeling study of pH and related solutes in an irrigated anoxic coastal sediment. J. Mar. Res. **54:** 939–966.

OSINGA, R., A. J. KOP, G. C. A. DUINEVELD, R. A. PRINS, AND F. C. VAN DUYL. 1996. Benthic mineralization rates at two locations in the southern North Sea. J. Sea Res. **36:** 181–191.

PANKOW, H. 1990. Ostsee-Algenflora. Gustav-Fischer-Verlag.

PILDITCH, C. A., C. W. EMERSON, AND J. GRANT. 1998. Effect of scallop shells and sediment grain size on phytoplankton flux to the bed. Cont. Shelf Res. **17:** 1869–1885.

REISE, K. 1985. Tidal flat ecology. Springer.

———, E. HERRE, AND M. STURM. 1994. Biomass and abundance of macrofauna in intertidal sediments of Königshafen in the northern Wadden Sea. Helgol. Meeresunters. **48:** 201–215.

RICE, D. L., T. S. BIANCHI, AND E. H. ROPER. 1986. Experimental studies of sediment reworking and growth of *Scoloplos* spp. (Orbiniidae: Polychaeta). Mar. Ecol. Prog. Ser. **30:** 9–19.

RIEDL, R. J., N. HUANG, AND R. MACHAN. 1972. The subtidal pump, a mechanism of intertidal water exchange by wave action. Mar. Biol. **13:** 210–221.

ROCHA, C. 1998. Rhythmic ammonium regeneration and flushing in intertidal sediments of the Sado estuary. Limnol. Oceanogr. **43:** 823–831.

SACHS, L. 1997. Angewandte Statistik, 8th ed. Springer.

SHUM, K. T. 1995. A numerical study of the wave-induced solute transport above a rippled bed. J. Fluid Mech. **299:** 267–288.

———, AND B. SUNDBY. 1996. Organic matter processing in continental shelf sediments—the subtidal pump revisited. Mar. Chem. **53:** 81–87.

UPTON, A. C., D. B. NEDWELL, R. J. PARKES, AND S. M. HARVEY. 1993. Seasonal benthic microbial activity in the southern North Sea: Oxygen uptake and sulphate reduction. Mar. Ecol. Prog. Ser. **101:** 273–281.

VAN RAAPHORST, W., H. MALSCHAERT, AND H. VAN HAREN. 1998. Tidal resuspension and deposition of particulate matter in the Oyster Grounds, North Sea. J. Mar. Res. **56:** 257–291.

WEBB, D. G., AND P. A. MONTAGNA. 1993. Initial burial and subsequent degradation of sedimented phytoplankton—relative impact of macrobenthos and meiobenthos. J. Exp. Mar. Biol. Ecol. **166:** 151–163.

WHEATCROFT, R. A., P. A. JUMARS, C. R. SMITH, AND A. R. M. NOWELL. 1990. A mechanistic view of the particulate biodiffusion coefficient: Step lengths, rest periods and transport directions. J. Mar. Res. **48:** 177–207.

ZIEBIS, W., S. FORSTER, M. HUETTEL, AND B. B. JØRGENSEN. 1996*a*. Complex burrows of the mud shrimp *Callianassa truncata* and their geochemical impact in the sea bed. Nature **382:** 619–622.

———, M. HUETTEL, AND S. FORSTER. 1996*b.* Impact of biogenic sediment topography on oxygen fluxes in permeable sediments. Mar. Ecol. Prog. Ser. **140:** 227–237.

Received: 10 September 1999
Accepted: 17 December 1999
Amended: 5 January 2000